Phase-Driven Precision Boost in Quantum Compression for Postselected Metrology

Aiham M. Rostom 0,1,2,* Saeed Haddadi 0,3,† and Vladimir A. Tomilin²

¹Novosibirsk State University, 630090, Novosibirsk, Russia
²Institute of Automation and Electrometry SBRAS, 630090, Novosibirsk, Russia
³School of Particles and Accelerators, Institute for Research in Fundamental Sciences (IPM), P.O. Box 19395-5531, Tehran, Iran

We unveil the noncyclic Pancharatnam phase as a fundamental geometric criterion governing the optimal operation of quantum compression channels in postselected metrology. Harnessing this phase enables precise control over the interplay between orthogonal parameter sensitivity and parallel evolution in the meter state, thereby maximizing the quantum Fisher information per trial. Strikingly, fine-tuning the postselection parameter just below this optimal phase incurs substantial information loss, whereas tuning it just above fully suppresses undesired parallel evolution and boosts information retention by more than a tenfold factor relative to conventional approaches. We further reveal that leveraging qudit meter states can unlock a substantial additional quantum advantage. These findings establish the Pancharatnam phase as an essential and robust geometric benchmark, guiding the design of next-generation high-precision quantum parameter estimation protocols under realistic experimental constraints.

I. INTRODUCTION

Harnessing quantum correlations, quantum metrology enables parameter estimation at sensitivities unattainable by classical methods, with broad implications for foundational physics and advanced measurement applications [1–5]. Compression channels in postselected quantum metrology, wherein measurement outcomes are conditioned on specific postselection events, have emerged as a powerful paradigm for amplifying weak signals and enhancing sensitivity, offering a genuine quantum advantage [6–8].

Ouantum compression channels that utilize postselection protocols offer a range of significant technical advantages for enhancing precision of quantum metrology. Among these is the effective amplification of the input quanta flux in systems characterized by low generation rates, achieved through the recycling of unpostselected quantum resources [9]. Postselection inherently circumvents detector saturation by selectively heralding rare events [10], thereby mitigating nonlinear detector response and dead-time limitations. Moreover, the exploitation of postselection frameworks enhances the discrimination fidelity between genuine single photons, substantially suppressing detector noise contributions and elevating measurement sensitivity [11, 12]. Beyond these operational benefits, postselection engenders profound foundational phenomena, notably, the emergence of closed timelike curves within certain quantum circuit architectures [13, 14]. Recent theoretical and experimental investigations have illuminated the capacity of such non-classical causal structures to confer metrological advantages that surpass classical bounds [15], opening new avenues for exploiting temporal quantum correlations in parameter estimation.

Compression quantum channels enable more efficient and robust quantum metrology by allowing information to be concentrated into fewer, higher-quality measurement outcomes that are particularly valuable when measurements are expensive or noisy [6, 11]. However, the intrinsic probabilistic nature of postselection introduces challenges in efficiently compressing and transfer-

ring information from the quantum system to the measurement apparatus [6–8, 16–18]. Addressing this challenge requires identifying the optimal operational parameters that maximize the retention of quantum Fisher information (QFI) per trial, a central figure of merit quantifying achievable precision [6].

In this work, we unveil a fundamentally geometric solution to this problem by demonstrating that the operation on the noncyclic Pancharatnam phase uniquely optimizes the quality of quantum compression channels.

The Pancharatnam phase, originally introduced in the context of geometric phases for polarized light [19] and later extended to general quantum evolutions [20], prescribes a phase relation that captures the intrinsic geometry of quantum state transformations. Its robustness and operational significance have been verified theoretically and experimentally using interferometric and polarimetric methods [21–24]. Although the Pancharatnam phase has been extensively studied, its role in optimizing quantum compression channels remains unexplored.

In the following section, we derive the QFI associated with the system—meter interaction parameter as an explicit function of the channel operator. We then specify the channel and meter operators, expressing the QFI accordingly. Building on this foundation, the Discussion section presents the derivation of the Pancharatnam phase that characterizes the quantum channel and establishes the parallel transport condition necessary to control the unwanted parallel evolution of the meter state. Finally, we explore the optimality of the Pancharatnam phase as a natural parameterization for quantum compression channels, considering general qudit-meter states.

II. PRELIMINARIES

A. System-Meter Coupling and Channel Operator

Consider a quantum system described by the Hilbert space $\mathcal{H}_s = \mathrm{span}\left\{|\mathcal{S}_1\rangle, |\mathcal{S}_2\rangle, \dots, |\mathcal{S}_f\rangle, \dots\right\}$, initially prepared in state $|\mathcal{S}_i\rangle$. Suppose an ancillary system—the meter—initially in the state $|\mathcal{M}_i\rangle$. Assuming the system and meter are initially unentangled, their joint initial state is described by the tensor product

$$|\Psi_i\rangle = |\mathcal{S}_i\rangle \otimes |\mathcal{M}_i\rangle. \tag{1}$$

^{*} a.rostom@g.nsu.ru

[†] haddadi@ipm.ir

Suppose an evolution operator $\hat{\mathbb{J}}_{\lambda}(\Theta)$ acting on the combined system-meter Hilbert space, where Θ denotes an experimentally tunable postselection parameter controlling the quantum system. The joint state is given by

$$|\Psi_{\lambda}(\Theta)\rangle = \hat{\mathbb{J}}_{\lambda}(\Theta)|\mathcal{S}_{i}\rangle \otimes |\mathcal{M}_{i}\rangle.$$
 (2)

By postselecting the system in the final state $|S_f\rangle$, the output conditional state becomes

$$|\Psi_{\lambda}(\Theta)\rangle \propto (|\mathcal{S}_f\rangle\langle\mathcal{S}_f| \otimes \hat{\mathbb{I}})\hat{\mathbb{J}}_{\lambda}(\Theta) |\mathcal{S}_i\rangle \otimes |\mathcal{M}_i\rangle$$

= $|\mathcal{S}_f\rangle \otimes \hat{\mathbb{K}}_{\lambda}(\Theta)|\mathcal{M}_i\rangle,$ (3)

where $\hat{\mathbb{K}}_{\lambda}(\Theta) = \langle \mathcal{S}_f | \hat{\mathbb{J}}_{\lambda}(\Theta) | \mathcal{S}_i \rangle$ is the channel operator, representing an effective transformation acting solely on the meter state. Under the action of $\hat{\mathbb{K}}_{\lambda}(\Theta)$, the output normalized state

$$|\Psi_{\lambda}(\Theta)\rangle = \mathcal{P}_{\lambda}^{-1/2}(\Theta)|\mathcal{S}_f\rangle \otimes \hat{\mathbb{K}}_{\lambda}(\Theta)|\mathcal{M}_i\rangle,$$
 (4)

exhibits an amplified sensitivity to weak-coupling strengths λ . The normalization function $\mathcal{P}_{\lambda}(\Theta)$ determines the postselection probability

$$\mathcal{P}_{\lambda}(\Theta) = \langle \mathcal{M}_i | \hat{\mathbb{K}}_{\lambda}^{\dagger}(\Theta) \hat{\mathbb{K}}_{\lambda}(\Theta) | \mathcal{M}_i \rangle = \langle \hat{\mathbb{K}}_{\lambda}^{\dagger}(\Theta) \hat{\mathbb{K}}_{\lambda}(\Theta) \rangle. \tag{5}$$

B. QFI: Total and Parallel Evolution Characterized by $\hat{\mathbb{K}}_{\lambda}(\Theta)$

In this subsection, we analyze the total and parallel contributions to the QFI as expressed through the operator $\hat{\mathbb{K}}_{\lambda}(\Theta)$

QFI quantifies the sensitivity of the quantum state $|\Psi_{\lambda}\rangle$ to changes in the parameter λ and sets the theoretical limits for estimation precision via the quantum Cramér-Rao bound

$$\mathbf{Var}(\lambda) \ge \frac{1}{M \cdot \mathcal{I}_{\lambda}^{\perp}},\tag{6}$$

where M is the number of measurements and $\mathcal{I}_{\lambda}^{\perp}$ is the observed QFI of a single measurement. QFI is a gauge-invariant quantity (Appendix C), as it depends only on the orthogonal component $|\partial_{\lambda}\Psi_{\lambda}^{\perp}\rangle$ (Appendix B)

$$\begin{split} \mathcal{I}_{\lambda}^{\perp} &= 4 \big\| |\partial_{\lambda} \Psi_{\lambda}^{\perp} \rangle \big\|^{2} = 4 \big(\langle \partial_{\lambda} \Psi_{\lambda} | \partial_{\lambda} \Psi_{\lambda} \rangle - |\langle \Psi_{\lambda} | \partial_{\lambda} \Psi_{\lambda} \rangle|^{2} \big) \\ &= 4 \big(\big\| |\partial_{\lambda} \Psi_{\lambda} \rangle \big\|^{2} - \big\| |\partial_{\lambda} \Psi_{\lambda}^{\parallel} \rangle \big\|^{2} \big) \\ &= \mathcal{I}_{\lambda}^{T} - \mathcal{I}_{\lambda}^{\parallel}. \end{split} \tag{7}$$

The term $\left\| |\partial_\lambda \Psi_\lambda \rangle \right\|^2$ quantifies the total rate of change of the quantum state $|\Psi_\lambda \rangle$ in Hilbert space with respect to the parameter λ . The second term corresponds to the parallel component $|\partial_\lambda \Psi_\lambda^\parallel \rangle$ —a gauge-dependent contribution and thus does not contribute to physically accessible information.

By substituting the postselected state $|\Psi_{\lambda}(\Theta)\rangle$, the QFI under postselection becomes (Appendix D)

$$\mathcal{I}_{\lambda}^{\perp}(\Theta) = 4\mathcal{P}_{\lambda}^{-2}(\Theta) [\mathcal{Q}_{\lambda}^{T}(\Theta).\mathcal{P}_{\lambda}(\Theta) - \mathcal{Q}_{\lambda}^{\parallel}(\Theta)], \tag{8}$$

where $\mathcal{Q}_{\lambda}^{T}(\Theta) = \langle \partial_{\lambda} \hat{\mathbb{K}}_{\lambda}^{\dagger}(\Theta) \partial_{\lambda} \hat{\mathbb{K}}_{\lambda}(\Theta) \rangle$ is the average total change in the channel operator with respect to the parameter λ , and $\mathcal{Q}_{\lambda}^{\parallel}(\Theta) = |\langle \hat{\mathbb{K}}_{\lambda}^{\dagger}(\Theta) \partial_{\lambda} \hat{\mathbb{K}}_{\lambda}(\Theta) \rangle|^{2}$ is its parallel evolution. The parallel component here is not simply subtracted as a gauge artifact but interacts nontrivially with \mathcal{P}_{λ} .

C. QFI Yield per Trial

The maximum QFI per trial (without postselection) is $(\Delta u)^2$ [6], where Δu denotes the difference between the largest and smallest eigenvalues of the system's generator for the unitary transformation encoding the parameter λ . The quantum advantage gained via postselection is quantified by the total QFI per trial [6]

$$\mathcal{T}(\Theta) = \mathcal{P}_{\lambda}(\Theta)\mathcal{I}_{\lambda}^{\perp}(\Theta) > \left(\Delta u\right)^{2},\tag{9}$$

which serves as the central metric for evaluating the efficiency of the compression channel. This metric balances high precision—potentially large $\mathcal{I}_{\lambda}^{\perp}(\Theta)$ —against the typically reduced success probability $\mathcal{P}_{\lambda}(\Theta)$ arising from postselection on rare events [25].

Our main objective is two-fold: to determine the postselection parameter Θ_{\perp} that maximizes $\mathcal{I}_{\lambda}^{\perp}(\Theta)$, and, more crucially, to identify the optimal postselection parameter Θ_{\parallel} that satisfies $\mathcal{Q}_{\lambda}^{\parallel}=0$, where all parameter-induced changes are encoded fully in physically distinguishable directions in Hilbert space. This is a necessary condition for maximizing \mathcal{T} as we will demonstrate below.

III. DETERMINATION OF THE CHANNEL OPERATOR $\hat{\mathbb{K}}_{\lambda}(\Theta)$

Consider a quantum system described by a two-mode Hilbert space, whose structure can be elegantly and compactly captured through the Jordan–Schwinger map [26]

$$\hat{J}_{x} = \frac{1}{2} (\hat{a}_{1}^{\dagger} \hat{a}_{2} + \hat{a}_{2}^{\dagger} \hat{a}_{1}), \quad \hat{J}_{y} = \frac{i}{2} (\hat{a}_{2}^{\dagger} \hat{a}_{1} - \hat{a}_{1}^{\dagger} \hat{a}_{2}),$$

$$\hat{J}_{z} = \frac{1}{2} (\hat{a}_{1}^{\dagger} \hat{a}_{1} - \hat{a}_{2}^{\dagger} \hat{a}_{2}), \quad \hat{J}_{t} = \frac{1}{2} (\hat{a}_{1}^{\dagger} \hat{a}_{1} + \hat{a}_{2}^{\dagger} \hat{a}_{2}).$$
(10)

where $(\hat{a}_1^{\dagger}, \hat{a}_2^{\dagger})$ and (\hat{a}_1, \hat{a}_2) are creation and annihilation operators, respectively. These operators form a closed algebra under the commutator bracket, satisfying $[\hat{J}_i, \hat{J}_j] = i \epsilon_{ijk} \hat{J}_k$, where ϵ_{ijk} is the Levi-Civita symbol, and \hat{J}_t commutes with all other \hat{J}_i .

The system–meter interaction is commonly modeled by a Hamiltonian that couples the meter to one or more system observables. The total Hilbert space for the combined system is given by the tensor product $\mathcal{H} = \mathcal{H}_{\mathcal{S}} \otimes \mathcal{H}_{\mathcal{M}}$, where $\mathcal{H}_{\mathcal{S}}$ and $\mathcal{H}_{\mathcal{M}}$ denote the Hilbert spaces of the system and the meter, respectively. The interaction dynamics can be described by the unitary operator

$$\hat{\Lambda} = \exp\left[i\lambda \left(\hat{J}_t^{(\mathcal{S})} + \hat{J}_z^{(\mathcal{S})}\right) \otimes \hat{\mathcal{U}}^{(\mathcal{M})}\right],\tag{11}$$

where $\hat{\mathcal{U}}^{(\mathcal{M})}$ is a Hermitian operator acting on the meter's state. The operator \hat{A} encapsulates the interaction between the system's mode 2 and the meter. Incorporating a controlled phase applied to mode 1, the overall operator governing the system's evolution is then defined as

$$\hat{\mathbb{J}}_{\lambda}(\Theta) = \left[e^{-i\frac{\pi}{2}\hat{J}_{x}^{(\mathcal{S})}} \otimes \hat{\mathbb{I}}^{(\mathcal{M})}\right] \left[e^{i\Theta\left(\hat{J}_{t}^{(\mathcal{S})} - \hat{J}_{z}^{(\mathcal{S})}\right)} \otimes \hat{\mathbb{I}}^{(\mathcal{M})}\right] \times \hat{\Lambda} \left[e^{+i\frac{\pi}{2}\hat{J}_{x}^{(\mathcal{S})}} \otimes \hat{\mathbb{I}}^{(\mathcal{M})}\right]. \tag{12}$$

The operator $e^{\pm i \frac{\pi}{2} \hat{J}_x^{(\mathcal{S})}}$ generates a rotation about the x-axis, effectively implementing the 50:50 splitting and recombination of the two quantum modes. Using the identity $\hat{U}e^{\hat{A}}\hat{U}^{\dagger}=e^{\hat{U}\hat{A}\hat{U}^{\dagger}}$, and Baker-Campbell-Haussdorff relations $e^{-i \frac{\pi}{2} \hat{J}_x^{(\mathcal{S})}} \hat{J}_z^{(\mathcal{S})} e^{+i \frac{\pi}{2} \hat{J}_x^{(\mathcal{S})}} = -\hat{J}_y^{(\mathcal{S})}, \ e^{-i \frac{\pi}{2} \hat{J}_x^{(\mathcal{S})}} \hat{J}_t^{(\mathcal{S})} e^{+i \frac{\pi}{2} \hat{J}_x^{(\mathcal{S})}} = \hat{J}_t^{(\mathcal{S})}$, the operator $\hat{\mathbb{J}}_{\lambda}(\Theta)$ can be expressed as

$$\hat{\mathbb{J}}_{\lambda}(\Theta) \to \left[e^{i\Theta\left(\hat{J}_{t}^{(\mathcal{S})} + \hat{J}_{y}^{(\mathcal{S})}\right)} \otimes \hat{\mathbb{I}}^{(\mathcal{M})}\right] e^{i\lambda\left(\hat{J}_{t}^{(\mathcal{S})} - \hat{J}_{y}^{(\mathcal{S})}\right)} \otimes \hat{\mathcal{U}}^{(\mathcal{M})}. \tag{13}$$

The pre- and postselected states can be chosen to be $(|S_i\rangle = |j, m_i\rangle$ and $|S_f\rangle = |j, m_f\rangle$), where

$$|j,m\rangle \equiv |n_1,n_2\rangle = \frac{(a_1^\dagger)^{j+m}(a_2^\dagger)^{j-m}}{\sqrt{(j+m)!(j-m)!}}|0,0\rangle,$$

where $j=\frac{n_1+n_2}{2}$ is the total angular momentum quantum number, $m=\frac{n_1-n_2}{2}$ is the eigenvalue of \hat{J}_z (the magnetic quantum number), and $|0,0\rangle$ is the vacuum state. Consequently, the operator $\hat{\mathbb{K}}_{\lambda}(\Theta)$, can be obtained by projecting $\hat{\mathbb{J}}_{\lambda}(\Theta)$ onto the pre- and postselected states, yielding

$$\hat{\mathbb{K}}_{\lambda}^{(j)}(\Theta) = \langle \mathcal{S}_f | \hat{\mathbb{J}}_{\lambda}(\Theta) | \mathcal{S}_i \rangle
= \langle j, m_f | \hat{\mathbb{J}}_{\lambda}(\Theta) | j, m_i \rangle
= e^{ij\Theta} e^{ij\lambda\hat{\mathcal{U}}^{(\mathcal{M})}} \hat{\mathcal{F}}_{m_f, m_i}^{(j)} (\Theta \hat{\mathbb{I}}^{(\mathcal{M})} - \lambda \hat{\mathcal{U}}^{(\mathcal{M})}),$$
(14)

where $\hat{J}_t^{(\mathcal{S})}|j,m_i\rangle=j|j,m_i\rangle,\,\hat{J}_z^{(\mathcal{S})}|j,m\rangle=m|j,m\rangle$ and

$$\hat{\mathcal{F}}_{m_f,m_i}^{(j)} \left(\Theta - \lambda \hat{\mathcal{U}}^{(\mathcal{M})} \right) = \langle j, m_f | e^{i\hat{J}_y^{(\mathcal{S})} \otimes \left(\Theta \hat{\mathbb{I}}^{(\mathcal{M})} - \lambda \hat{\mathcal{U}}^{(\mathcal{M})} \right)} | j, m_i \rangle. \tag{15}$$

Applying $\hat{\mathcal{F}}_{m_f,m_i}^{(j)}$ on the meter eigenstate $|k\rangle$ of the operator $\hat{\mathcal{U}}^{(\mathcal{M})}$ gives

$$\hat{\mathcal{F}}_{m_f,m_i}^{(j)}(\Theta - \lambda \hat{\mathcal{U}}^{(\mathcal{M})})|k\rangle = d_{m_f,m_i}^{(j)}(\Theta - u_k \lambda)|k\rangle,$$

where $d_{m_f,m_i}^{(j)}(\Theta - u_k \lambda)$ is the Wigner d-matrix element that corresponds to the eigenvalues u_k of the meter operator $\hat{\mathcal{U}}^{(\mathcal{M})}$.

A. General Meter Operators

Here, we present a mathematical formula that facilitates the determination of the channel operator $\hat{\mathbb{K}}_{\lambda}^{(j)}(\Theta)$ for an arbitrary meter state.

The states $|j,m_i\rangle$ and $|j,m_f\rangle$ considered above are eigenstates of $\hat{J}_z^{(\mathcal{S})}$, and the operators $\hat{\mathbb{I}}^{(\mathcal{M})}$ and $\hat{\mathcal{U}}^{(\mathcal{M})}$ act solely on the meter state. To evaluate the matrix element $\hat{\mathcal{F}}_{m_f,m_i}^{(j)}\left(\Theta\hat{\mathbb{I}}^{(\mathcal{M})}-\lambda\hat{\mathcal{U}}^{(\mathcal{M})}\right)$, we first express the system states in the eigenbasis of $\hat{J}_y^{(\mathcal{S})}$ using the Wigner d-matrix

$$|j,m\rangle = \sum_{m_y=-j}^{j} d_{m_y,m}^{(j)}(\pi/2)|j,m_y\rangle,$$
 (16)

where $d_{m_y,m}^{(j)}(\pi/2)$ is the Wigner d-matrix element for a rotation by angle $\pi/2$ about the y-axis. The operator

$$\exp[i\,\hat{J}_y^{(\mathcal{S})} \otimes (\Theta\,\hat{\mathbb{I}}^{(\mathcal{M})} - \lambda\,\hat{\mathcal{U}}^{(\mathcal{M})})] \tag{17}$$

acts diagonally in this basis, yielding eigenvalues m_y for $\hat{J}_y^{(\mathcal{S})}$, so that its action on $|j,m_y\rangle$ is simply a multiplication by $\exp[i\,m_y(\Theta\,\hat{\mathbb{I}}^{(\mathcal{M})}-\lambda\,\hat{\mathcal{U}}^{(\mathcal{M})})]$. Substituting the expansions for both $|j,m_i\rangle$ and $|j,m_f\rangle$, and using the orthogonality of the \hat{J}_y eigenstates, the matrix element reduces to a sum over products of Wigner d-matrix elements and the exponential operator

$$\hat{\mathcal{F}}_{m_f,m_i}^{(j)} \left(\Theta \hat{\mathbb{I}}^{(\mathcal{M})} - \lambda \hat{\mathcal{U}}^{(\mathcal{M})} \right) = \sum_{m_y = -j}^{j} d_{m_y,m_f}^{(j)} \left(\frac{\pi}{2} \right) d_{m_y,m_i}^{(j)} \left(\frac{\pi}{2} \right) \times e^{im_y (\Theta \hat{\mathbb{I}}^{(\mathcal{M})} - \lambda \hat{\mathcal{U}}^{(\mathcal{M})})}.$$
(18)

where the sum runs over all eigenvalues m_y of $\hat{J}_y^{(\mathcal{S})}$. This construction relates the matrix element $\hat{\mathcal{F}}_{m_f,m_i}^{(j)}$ to a weighted sum over all possible projections onto the \hat{J}_y eigenbasis, with each term governed by the system's rotation properties and the meter operator.

B. Qudit Meter State

Alternatively, we consider a specific yet sufficiently general qudit meter state $|\mathcal{M}_i\rangle = |\mathcal{M}_d^{(n)}\rangle = \frac{1}{\sqrt{d}}\sum_{k=0}^{d-1}|b_k\rangle^{\otimes n}$, for n subsystems and d-dimensional Hilbert space, where $\mathcal{B} = \{|b_0\rangle, |b_1\rangle, ..., |b_{d-1}\rangle\}$ is an orthonormal basis. The meter operator can be defined as

$$e^{i\lambda\hat{\mathcal{U}}^{(\mathcal{M})}} = \left[\sum_{k=0}^{d-1} e^{iu_k\lambda} |b_k\rangle\langle b_k|\right]^{\otimes n},\tag{19}$$

which imprints a mode-dependent relative phase $e^{inu_k\lambda}$ on each component $|b_k\rangle^{\otimes n}$, yielding

$$e^{ij\lambda\hat{\mathcal{U}}^{(\mathcal{M})}}|\mathcal{M}_d^{(n)}\rangle = \frac{1}{\sqrt{d}}\sum_{k=0}^{d-1}e^{ijnu_k\lambda}|b_k\rangle^{\otimes n}.$$
 (20)

This ensures a phase sensitivity of the meter state scales linearly with the number of subsystems n. The operator $e^{i\lambda\hat{\mathcal{U}}^{(\mathcal{M})}}$ reduces to the familiar single-qubit phase gate in the case d=2, n=1, thus providing a natural generalization to multipartite, high-dimensional entangled meter states. By acting on $|\mathcal{M}_d^{(n)}\rangle$ using the channel operator we get

$$\hat{\mathbb{K}}_{\lambda}^{(j)}(\Theta)|\mathcal{M}_{d}^{(n)}\rangle = \frac{e^{ij\Theta}}{\sqrt{d}} \sum_{k=0}^{d-1} e^{ijnu_{k}\lambda} d_{m_{f},m_{i}}^{(j)}(\beta_{k})|b_{k}\rangle^{\otimes n}, \quad (21)$$

where $\beta_k = \Theta - nu_k \lambda$. Thus, the postselection probability gives

$$\mathcal{P}_{\lambda}^{(j)}(\Theta) = \frac{1}{d} \sum_{k=0}^{d-1} \left[d_{m_f, m_i}^{(j)}(\beta_k) \right]^2, \tag{22}$$

here the squared d-matrix elements quantify the transition probabilities between the states $|j,m_i\rangle$ and $|j,m_f\rangle$ induced by a rotation through the angle β_k . Averaging these elements over d terms reflects a uniform sampling of the rotation parameter β_k , ensuring an unbiased characterization. For the Wigner

d-matrix $\sum_{m_f} d_{m_f,m_i}^{(j)}(\beta_k).d_{m_f,m_j}^{(j)}(\beta_k) = \delta_{m_i,m_j}$, and hence $\sum_{m_f} \left[d_{m_f,m_i}^{(j)}(\beta_k) \right]^2 = 1$, which confirms that $\sum_{m_f} \mathcal{P}_{\lambda}^{(j)}(\Theta) = 1$

Taking the derivative of Eq. (21) with respect to the parameter λ gives

$$\partial_{\lambda} \hat{\mathbb{K}}_{\lambda}^{(j)}(\Theta) | \mathcal{M}_{d}^{(n)} \rangle = \frac{n e^{ij\Theta}}{\sqrt{d}} \sum_{k=0}^{d-1} u_{k} e^{ijnu_{k}\lambda} A_{k} | b_{k} \rangle^{\otimes n}, \quad (23)$$

where $A_k:=ijd_{m_f,m_i}^{(j)}(\beta_k)-\frac{d}{d\beta}d_{m_f,m_i}^{(j)}(\beta)\Big|_{\beta=\beta_k}$. The total change in the channel operator captured by \mathcal{Q}_{λ}^T can subsequently be expressed as

$$\mathcal{Q}_{\lambda}^{T} = \frac{n^{2}}{d} \sum_{k=0}^{d-1} \sum_{k'=0}^{d-1} u_{k} u_{k'} e^{-ijnu_{k'}\lambda} e^{ijnu_{k}\lambda}$$

$$\times A_{k} A_{k'}^{*} \langle b_{k'} |^{\otimes n} | b_{k} \rangle^{\otimes n}$$

$$= \frac{n^{2}}{d} \sum_{k=0}^{d-1} u_{k}^{2} |A_{k}|^{2},$$
(24)

where $\langle b_{k'}|^{\otimes n}|b_k\rangle^{\otimes n}=\delta_{k,k'}.$ Equivalently, the parallel term takes the form

$$Q_{\lambda}^{\parallel}(\Theta) = \frac{n^2}{d^2} \left| \sum_{k=0}^{d-1} u_k d_{m_f, m_i}^{(j)}(\beta_k) . A_k \right|^2.$$
 (25)

IV. RESULTS AND DISCUSSION

We base our discussion on pre- and postselecting the highest and lowest weight states, respectively, denoted by $|j,m_i\rangle=|j,j\rangle$, and $|j,m_f\rangle=|j,-j\rangle$. The corresponding Wigner d-matrix element is given by $d_{-j,j}^{(j)}(\beta_k)=\left[\sin\left(\frac{\beta_k}{2}\right)\right]^{2j}$. The expressions given in (22), (24), and (25) can then be, respectively, rewritten as

$$\mathcal{P}_{\lambda}^{(j)} = \frac{1}{d} \sum_{k=0}^{d-1} \left[\sin\left(\frac{\beta_k}{2}\right) \right]^{4j}, \tag{26}$$

$$Q_{\lambda}^{T} = \frac{4n^{2}j^{2}}{d} \sum_{k=0}^{d-1} u_{k}^{2} \sin^{4j-2}\left(\frac{\beta_{k}}{2}\right), \tag{27}$$

$$Q_{\lambda}^{\parallel} = \frac{4n^2j^2}{d^2} \left| \sum_{k=0}^{d-1} u_k \sin^{4j-1}\left(\frac{\beta_k}{2}\right) e^{i\frac{nu_k\lambda}{2}} \right|^2.$$
 (28)

representing the postselection probability, total and parallel changes.

A. Characterizing Quantum Compression Channels via the Pancharatnam Phase

In this section, we demonstrate that, for a general meter state, the postselected system operates as an interferometric setup exhibiting characteristic Pancharatnam phase effects. From Eq. (18), the matrix element $\mathcal{F}_{m_k,m_i}^{(j)}(\Theta - \hat{\mathcal{U}}_{\lambda}^{(\mathcal{M})})$ can be written as a finite sum of exponentials in Θ and $\hat{\mathcal{U}}_{\lambda}^{(\mathcal{M})}$ for any spin-j. Correspondingly, the channel operator (14) yields

$$\hat{\mathbb{K}}_{\lambda}^{(j)}(\Theta) = e^{ij\Theta} e^{ij\lambda\hat{\mathcal{U}}^{(\mathcal{M})}} \hat{\mathcal{F}}_{-j,j}^{(j)} \left(\Theta \hat{\mathbb{I}}^{(\mathcal{M})} - \lambda \hat{\mathcal{U}}^{(\mathcal{M})}\right)
= (-1)^{j} e^{ij\Theta} e^{ij\lambda\hat{\mathcal{U}}^{(\mathcal{M})}} \sin^{2j} \left(\frac{\Theta \hat{\mathbb{I}}^{(\mathcal{M})} - \lambda \hat{\mathcal{U}}^{(\mathcal{M})}}{2}\right)
= \frac{(-1)^{j}}{(2i)^{2j}} \left(e^{i\Theta} \hat{\mathbb{I}}^{(\mathcal{M})} - \hat{\mathcal{O}}_{\lambda}\right)^{2j},$$
(29)

where $\hat{\mathcal{O}}_{\lambda}=e^{i\lambda\hat{\mathcal{U}}^{(\mathcal{M})}}$, and the postselection probability is given by

$$\mathcal{P}_{\lambda}^{(j)}(\Theta) = \frac{1}{16^{j}} \left\langle \left(2\hat{\mathbb{I}}^{(\mathcal{M})} - e^{i\Theta} \hat{\mathcal{O}}_{\lambda}^{\dagger} - e^{-i\Theta} \hat{\mathcal{O}}_{\lambda} \right)^{2j} \right\rangle, \tag{30}$$

which represents a 2j-th order interference kernel that generates quantum fringes with phase sensitivity controlled by Θ , phase shift inherited from the eigenvalues of $\hat{\mathcal{O}}_{\lambda}$, and contrast scaling determined by j.

Since $\hat{\mathcal{O}}_{\lambda}$ is unitary, then $\hat{\mathcal{O}}_{\lambda}^{\dagger}\hat{\mathcal{O}}_{\lambda}=\hat{\mathbb{I}},\ \langle\hat{\mathcal{O}}_{\lambda}^{\dagger}\hat{\mathcal{O}}_{\lambda}\rangle=1$, and its expectation value satisfy: $\langle\hat{\mathcal{O}}_{\lambda}^{\dagger}\rangle=\langle\hat{\mathcal{O}}_{\lambda}\rangle^*$. Define $\langle\hat{\mathcal{O}}_{\lambda}\rangle=|\langle\hat{\mathcal{O}}_{\lambda}\rangle|\,e^{i\mathrm{Im}\ln\langle\hat{\mathcal{O}}_{\lambda}\rangle}$. The postselection probability for j=1/2 can be expressed as

$$\begin{split} \mathcal{P}_{\lambda}^{(1/2)}(\Theta) &= \frac{1}{4} \left(2 - e^{i\Theta} \left\langle \hat{\mathcal{O}}^{\dagger}(\lambda) \right\rangle - e^{-i\Theta} \left\langle \hat{\mathcal{O}}_{\lambda} \right\rangle \right) \\ &= \frac{1}{2} \left[1 - \left| \left\langle \hat{\mathcal{O}}_{\lambda} \right\rangle \right| \cos \left(\Theta - \operatorname{Im} \ln \left\langle \hat{\mathcal{O}}_{\lambda} \right\rangle \right) \right], \end{split} \tag{31}$$

where $|\langle \hat{\mathcal{O}}_{\lambda} \rangle|$ is the visibility, and Im $\ln \langle \hat{\mathcal{O}}_{\lambda} \rangle$ is Pancharatnam phase difference between the two system's modes [27]. In the context of postselected quantum metrology, it can be defined to be the phase by which one mode must be retarded or advanced to make the postselection probability in the system reach its minimum (see Appendix E for more details on the interpretation of this phase).

B. Parallel Transport and Θ -Optimization

To illustrate the optimization mechanism, the QFI can be conveniently reformulated in terms of the meter's interaction operators $\hat{\mathcal{O}}_{\lambda}$. In particular, for j=1/2, the first term, which corresponds to the total rate of change, can be expressed as

$$Q_{\lambda}^{T} = \frac{1}{4} \left\langle \partial_{\lambda} \hat{\mathcal{O}}_{\lambda}^{\dagger} . \partial_{\lambda} \hat{\mathcal{O}}_{\lambda} \right\rangle. \tag{32}$$

At the same time, the parallel term—arising from nonphysical phase variations—becomes

$$Q_{\lambda}^{\parallel}(\Theta) = \frac{1}{16} \left| \left\langle \partial_{\lambda} \hat{\mathcal{O}}_{\lambda} \right\rangle - e^{i\Theta} \left\langle \hat{\mathcal{O}}_{\lambda}^{\dagger} \partial_{\lambda} \hat{\mathcal{O}}_{\lambda} \right\rangle \right|^{2}. \tag{33}$$

Here $\mathcal{Q}_{\lambda}^{\parallel}(\Theta)$ originates from correlations between the parameter-encoding operator $\hat{\mathcal{O}}_{\lambda}$ and its derivative $\partial_{\lambda}\hat{\mathcal{O}}_{\lambda}$, modulated by the controllable phase Θ . Under parallel transport $(\langle\hat{\mathcal{O}}_{\lambda}^{\dagger}\partial_{\lambda}\hat{\mathcal{O}}_{\lambda}\rangle = 0$, see Appendices A and E), $\mathcal{Q}_{\lambda}^{\parallel}(\Theta)$ simplifies to $|\langle\partial_{\lambda}\hat{\mathcal{O}}_{\lambda}\rangle|^2$, reflecting orthogonal fluctuations determined by the magnitude of the derivative and unaffected by Θ .

Conversely, when parallel transport is not imposed, active suppression of $\mathcal{Q}_{\lambda}^{\parallel}(\Theta)$ becomes possible: by tuning Θ to align with the operator's intrinsic phase, $\mathcal{Q}_{\lambda}^{\parallel}(\Theta)$ can be driven to zero, thus surpassing the precision achievable under parallel transport $\langle \hat{\mathcal{O}}_{\lambda}^{\dagger} \partial_{\lambda} \hat{\mathcal{O}}_{\lambda} \rangle = 0$. We illustrate this point below in greater detail.

C. Meter Operator Design: Gauge Freedom Considerations

Here, we analyze two representative classes of meter states that critically shapes and maximizes the QFI.

The first is the computational basis, $|b_k\rangle=|k\rangle$, where the meter state can be defined as $|\mathcal{M}_d^{(n)}\rangle=\frac{1}{\sqrt{d}}\sum_{k=0}^{d-1}|k\rangle^{\otimes n}$. The corresponding meter operator is given by

$$\hat{\mathcal{O}}_{\lambda}^{P} = e^{i\lambda\hat{\mathcal{U}}^{(\mathcal{M})}} = \left[\sum_{k}^{d-1} e^{ik\lambda} |k\rangle\langle k|\right]^{\otimes n},\tag{34}$$

with the generator $\hat{\mathcal{U}}^{(\mathcal{M})}=\hat{J}_t^{(\mathcal{M})}+\hat{J}_z^{(\mathcal{M})}$. We denote this meter operator by $\hat{\mathcal{O}}_{\lambda}^P$ to emphasize its role as the generator of the Pancharatnam phase

$$\operatorname{Im} \ln \langle \hat{\mathcal{O}}_{\lambda}^{P} \rangle = \operatorname{Im} \operatorname{Ln} \left(\sum_{k=0}^{d-1} e^{ink\lambda} \right) = n \frac{(d-1)\lambda}{2}. \tag{35}$$

This operator enables efficient Θ -optimization of $\mathcal{Q}_{\lambda}^{\parallel}(\Theta)$ through

$$\langle (\hat{\mathcal{O}}_{\lambda}^{P})^{\dagger} \partial_{\lambda} \hat{\mathcal{O}}_{\lambda}^{P} \rangle = \frac{1}{d} \sum_{k=0}^{d-1} \langle k |^{\otimes n} \left(\hat{\mathcal{O}}_{\lambda}^{P} \right)^{\dagger} \partial_{\lambda} \hat{\mathcal{O}}_{\lambda}^{P} | k \rangle^{\otimes n}$$
$$= in \frac{1}{d} \sum_{k=0}^{d-1} k = in \frac{d-1}{2} \neq 0. \tag{36}$$

The second case is the angular-momentum-basis, $|b_k\rangle=|\tilde{j},m_k\rangle$, where symbol \tilde{j} is used to distinguish it from the j of the postselected system. Here $m_k=k-\tilde{j}$ runs over all integer or half-integer values from $-\tilde{j}$ to \tilde{j} , and $\tilde{j}=\frac{d-1}{2}$. This yields

$$|\mathcal{M}_{d}^{(n)}\rangle = \frac{1}{\sqrt{d}} \sum_{k=0}^{d-1} |\tilde{j}, k - \tilde{j}\rangle^{\otimes n} = \frac{1}{\sqrt{d}} \sum_{m=-\tilde{j}}^{\tilde{j}} |\tilde{j}, m\rangle^{\otimes n}, \quad (37)$$

with the angular momentum basis being simply a reindexed computational basis. The meter operator in this case takes the form

$$\hat{\mathcal{O}}_{\lambda}^{(0)} = e^{i\lambda\hat{\mathcal{U}}^{(\mathcal{M})}} = \left[\sum_{m=-\tilde{j}}^{\tilde{j}} e^{im\lambda} |\tilde{j}, m\rangle \langle \tilde{j}, m|\right]^{\otimes n}$$
(38)

with the generator $\hat{\mathcal{U}}^{(\mathcal{M})}=\hat{J}_z^{(\mathcal{M})}$. We label this operator as $\hat{\mathcal{O}}_\lambda^{(0)}$ to indicate the absence of the Pancharatnam phase

$$\operatorname{Im} \ln \langle \hat{\mathcal{O}}_{\lambda}^{(0)} \rangle = \operatorname{Im} \operatorname{Ln} \left(\sum_{m=-\tilde{j}}^{\tilde{j}} e^{inm\lambda} \right) = 0. \tag{39}$$

The operator $\hat{\mathcal{O}}_{\lambda}^{(0)}$ obstructs the Θ -optimization of $\mathcal{Q}_{\lambda}^{\parallel}(\Theta)$ because

$$\langle (\hat{\mathcal{O}}_{\lambda}^{(0)})^{\dagger} \partial_{\lambda} \hat{\mathcal{O}}_{\lambda}^{(0)} \rangle = \frac{1}{d} \sum_{m = -\tilde{j}} \langle \tilde{j}, m |^{\otimes n} (\hat{\mathcal{O}}_{\lambda}^{(0)})^{\dagger} \partial_{\lambda} \hat{\mathcal{O}}_{\lambda}^{(0)} | \tilde{j}, m \rangle^{\otimes n}$$
$$= \frac{in}{d} \sum_{m = -\tilde{j}}^{\tilde{j}} m = 0. \tag{40}$$

As we shall see below, the QFI in the latter case is smaller than in the former. Remarkably, however, the two cases are physically equivalent with respect to the meter state, differing only by an overall phase factor. With the generators $\hat{\mathcal{U}}^{(\mathcal{M})} = \hat{J}_t^{(\mathcal{M})} + \hat{J}_z^{(\mathcal{M})}$ and $\hat{\mathcal{U}}^{(\mathcal{M})} = \hat{J}_z^{(\mathcal{M})}$ of $\hat{\mathcal{O}}_{\lambda}^{P}$ and $\hat{\mathcal{O}}_{\lambda}^{(0)}$ respectively, we write

$$\hat{\mathcal{O}}_{\lambda}^{P} = e^{i\lambda(\hat{J}_{t}^{(\mathcal{M})} + \hat{J}_{z}^{(\mathcal{M})})} = e^{i\lambda\hat{J}_{t}^{(\mathcal{M})}} e^{i\lambda\hat{J}_{z}^{(\mathcal{M})}} = e^{i\lambda\hat{J}_{t}^{(\mathcal{M})}} \hat{\mathcal{O}}_{\lambda}^{(0)}. \tag{41}$$

For a fixed dimension of the meter subspace, $\hat{J}_t^{(\mathcal{M})}$ acts as multiplication by a scalar \tilde{j} , contributing a global phase factor $e^{i\tilde{j}\lambda}$, independent of the basis states $|k\rangle$ or $|\tilde{j},m\rangle$. For example, when d=3 ($\tilde{j}=1$):

$$\hat{\mathcal{O}}_{\lambda}^{P} = \left[|0\rangle\langle 0| + e^{i\lambda}|1\rangle\langle 1| + e^{2i\lambda}|2\rangle\langle 2| \right]^{\otimes n}, \tag{42}$$

and

$$\hat{O}_{\lambda}^{(0)} = \left[e^{-i\lambda} |1, -1\rangle\langle 1, -1| + |1, 0\rangle\langle 1, 0| + e^{i\lambda} |1, 1\rangle\langle 1, 1| \right]^{\otimes n}
\equiv e^{-in\lambda} \left[|0\rangle\langle 0| + e^{i\lambda} |1\rangle\langle 1| + e^{2i\lambda} |2\rangle\langle 2| \right]^{\otimes n}
= e^{-in\lambda} \hat{\mathcal{O}}_{\lambda}^{P},$$
(43)

where $e^{-in\lambda}$ compensates for the index shift k=m+1. Considering the structure of the interaction unitary operator in Eq. (11), the operator \hat{O}^P_λ corresponds to an experimental scenario where a single system mode interacts with a single meter mode, whereas $\hat{O}^{(0)}_\lambda$ describes an interaction involving two meter modes. Notably, both operators generate the same relative phase in the meter state.

D. QFI Yield in Qudit-Qudit Coupling

Figure 1 presents contour plots of the total QFI per trial $\mathcal{T}=\mathcal{P}_{\lambda}^{(j)}(\Theta)\mathcal{I}_{\lambda}^{\perp}(\Theta)$ as a function of the coupling parameter λ and Θ , for various quantum numbers j. The results correspond to d=30, obtained directly from Eqs. (26), (27), and (28).

For j=1/2, the operator $\hat{\mathcal{O}}_{\lambda}^{P}$ displays a pronounced diagonal ridge even at small values of λ , indicating a significant enhancement in quantum sensitivity, $\mathcal{T}\gg \left(2j\right)^2$, along correlated values of λ and Θ . In contrast, the operator $\hat{\mathcal{O}}_{\lambda}^{(0)}$ exhibits a broad, symmetric maximum centered at small λ and intermediate Θ , decreasing rapidly outside this region. Overall, the quantum advantage in sensitivity achievable with $\hat{\mathcal{O}}_{\lambda}^{(0)}$ is notably limited compared to that of $\hat{\mathcal{O}}_{\lambda}^{P}$.

For higher values j=1,3/2, the landscape exhibits multiple local maxima and complex contour structures, with prominent high- \mathcal{T} regions occurring at intermediate parameter values. This

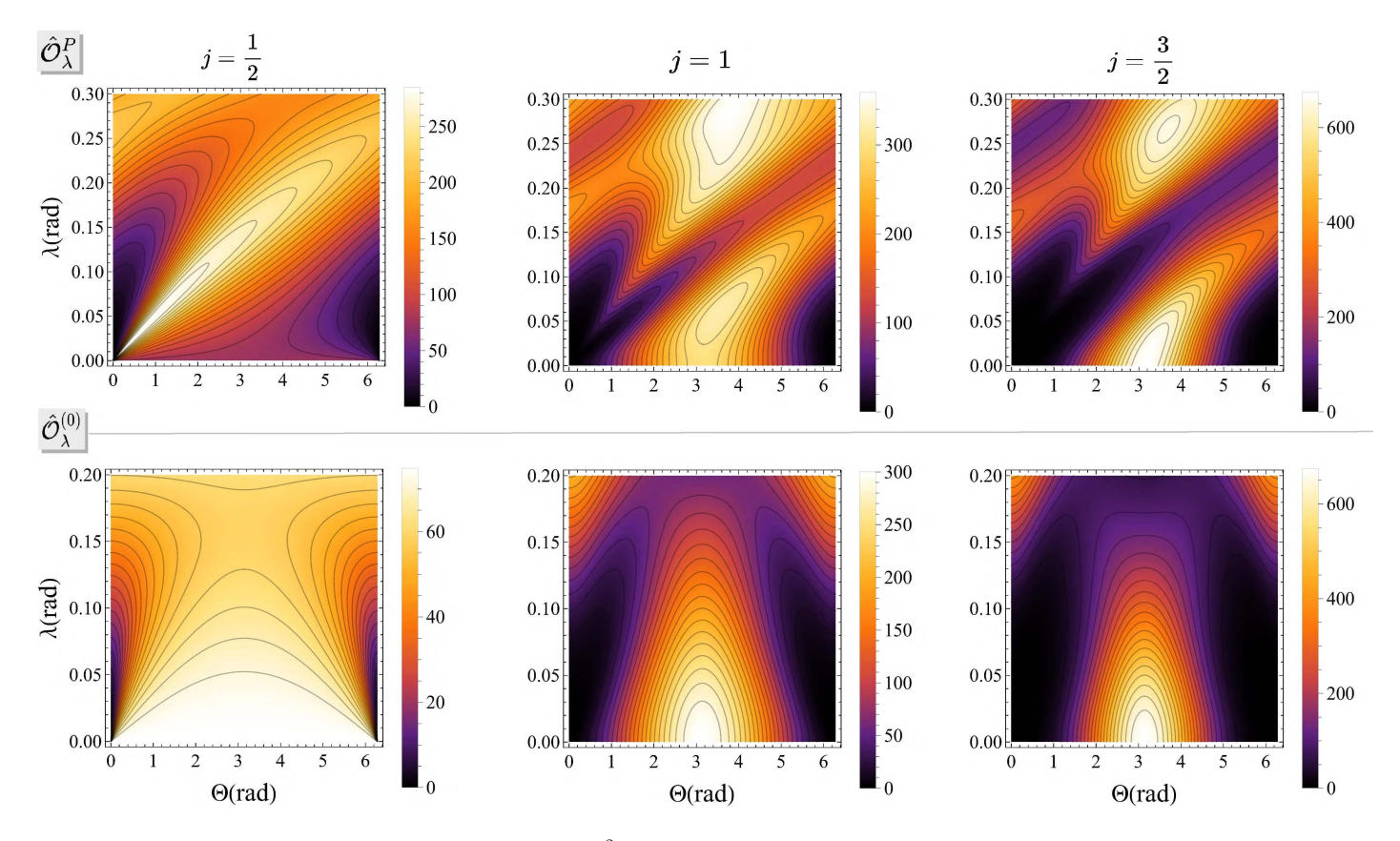


Figure 1. Contour plots of the normalized QFI per trial \mathcal{T}/n^2 depicted as functions of the coupling and postselection parameters λ and Θ , for quantum numbers j=1/2,1, and 3/2. The top row corresponds to calculations using the meter operator \hat{O}^P_{λ} , while the bottom row displays results obtained with $\hat{O}^{(0)}_{\lambda}$. In each panel, the color scale encodes the \mathcal{T} magnitude, with lighter shades indicating higher sensitivity. Further discussion and detailed physical interpretation are provided in the main text.

behavior highlights the suboptimality of the small (Θ, λ) regime as j increases, where $\mathcal{T} \ll \left(2j\right)^2$. This behavior arises because the QFI grows linearly with j (Eqs. (27) and (28)), while the postselection probability decreases exponentially

$$\mathcal{P}_{\lambda}^{(j)}(\Theta) = \frac{1}{2} \left\{ \left[\sin\left(\frac{\Theta}{2}\right) \right]^{4j} + \left[\sin\left(\frac{\Theta - n\lambda}{2}\right) \right]^{4j} \right\}$$

$$\approx \left[\mathcal{P}_{\lambda}^{(\frac{1}{2})}(\Theta) \right]^{2j}, \tag{44}$$

as shown in Fig. 2(a). $\mathcal T$ exhibits increasingly intricate features with pronounced peaks emerging at specific (Θ,λ) combinations, accompanied by an overall elevation in its maximal values. For smaller $\lambda,\mathcal T$ reaches its highest amplitudes near $\Theta\approx\pi$, corresponding to a high postselection probability. As the quantum number j increases, these peaks become increasingly localized around $\Theta\approx\pi$ and remain constrained to the regime of small and small λ .

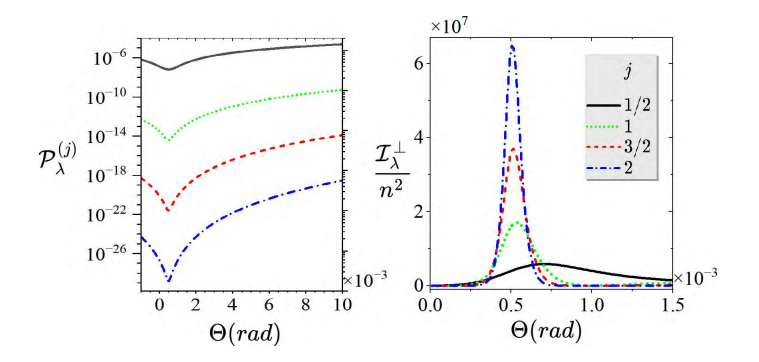
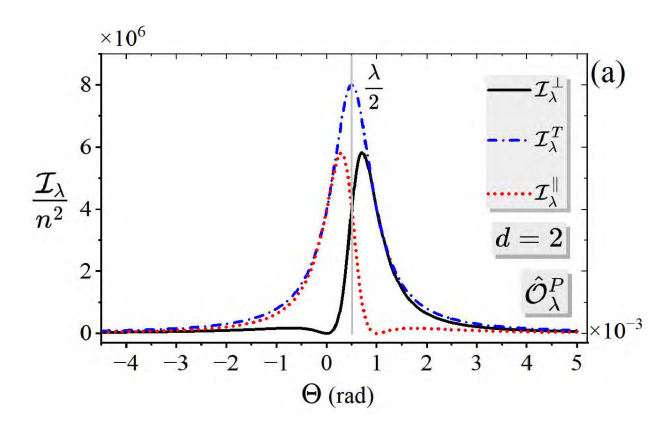


Figure 2. (a) The postselection probability, shifted by Pancharatnam phase $\frac{(d-1)n\lambda}{2}$, exhibits an exponential decay as the quantum number j increases. (b) The normalized QFI $\mathcal{I}_{\lambda}^{\perp}/n^2$ exhibits a linear growth as a function of j. Consequently, the total QFI per trial diminishes rapidly with increasing j in the weak-coupling regime. Notably, the QFI peak shifts towards the Pancharatnam phase as j increases. The results correspond to $n\lambda=10^{-3}$ and d=2.

These results underscore the fundamental dependence of \mathcal{T} on both the measurement operator's structure and the quantum number j. They reveal optimal parameter regimes for achieving superior quantum precision and elucidate the intricate interplay among coupling strength, the symmetry properties of the meter operator, and the dimensionality of the postselected system.



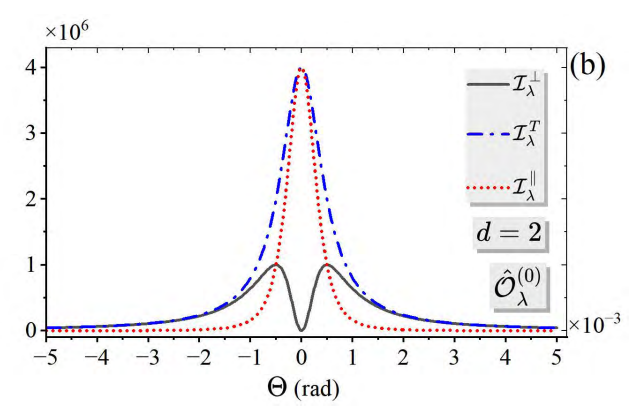


Figure 3. Normalized QFI $\mathcal{I}_{\lambda}^{\perp}/n^2$, $\mathcal{I}_{\lambda}^{T}/n^2$, and $\mathcal{I}_{\lambda}^{\parallel}/n^2$ as a function of Θ for $n\lambda=10^{-3}$ and d=2. (a) For the meter operator $\hat{\mathcal{O}}_{\lambda}^{P}$, the characteristic trade-off between $\mathcal{I}_{\lambda}^{\perp}(\Theta)$ and $\mathcal{I}_{\lambda}^{\parallel}(\Theta)$ occurs in the vicinity of the Pancharatnam phase $\frac{n\lambda}{2}$. (b) For the meter operator $\hat{\mathcal{O}}_{\lambda}^{(0)}$, both $\mathcal{I}_{\lambda}^{\parallel}(\Theta)$ and $\mathcal{I}_{\lambda}^{T}(\Theta)$ exhibit cooperative behavior, whereas the observable QFI $\mathcal{I}_{\lambda}^{\perp}(\Theta)$ suffers an approximately 83% reduction at $\Theta_{\perp}=\pm\frac{n\lambda}{2}$, indicating suboptimal performance of operator $\hat{\mathcal{O}}_{\lambda}^{(0)}$ in comparison with $\hat{\mathcal{O}}_{\lambda}^{p}$.

We conclude that notable technical advantages—characterized by a low postselection probability—and a high value of $\mathcal T$ are simultaneously attainable in the weak-coupling regime for j=1/2, corresponding to a two-level postselected system. In the following sections, we detail the Θ -optimization within this regime and demonstrate how the sensitivity can be further enhanced by employing a qudit meter.

E. QFI in the Special Case Of Qubit-Qubit Coupling

For d=2, the operator $\hat{\mathcal{O}}_{\lambda}^{P}$ then can be defined as

$$\hat{\mathcal{O}}_{\lambda}^{P} = |0\rangle\langle 0|^{\otimes n} + e^{in\lambda}|1\rangle\langle 1|^{\otimes n},\tag{45}$$

which imparts relative phase $n\lambda$ to the meter states. Given the meter initial state $|\mathcal{M}_2^{(n)}\rangle = \frac{1}{\sqrt{2}}(|0\rangle^{\otimes n} + |1\rangle^{\otimes n})$, the Pancharatnam phase is expressed as $\operatorname{Im} \ln \langle \hat{\mathcal{O}}_{\lambda}^{P} \rangle = n \frac{\lambda}{2}$, with the magnitude $|\langle \hat{\mathcal{O}}_{\lambda}^{P} \rangle| = |\cos(n \frac{\lambda}{2})|$. The orthogonal contribution associated with the total parameter variation is given by $\langle \partial_{\lambda} (\hat{\mathcal{O}}_{\lambda}^{P})^{\dagger} . \partial_{\lambda} \hat{\mathcal{O}}_{\lambda}^{P} \rangle = \frac{n^2}{2}$, while the term corresponding to parallel evolution reads

$$|\langle \partial_{\lambda} \hat{\mathcal{O}}_{\lambda}^{P} \rangle - e^{i\Theta} \langle (\hat{\mathcal{O}}_{\lambda}^{P})^{\dagger} . \partial_{\lambda} \hat{\mathcal{O}}_{\lambda}^{P} \rangle|^{2} = n^{2} \left| \sin(\frac{n\lambda - \Theta}{2}) \right|^{2}, \tag{46}$$

and the final QFI $\mathcal{I}_\lambda^\perp(\Theta)=\mathcal{I}_\lambda^T(\Theta)-\mathcal{I}_\lambda^\parallel(\Theta),$ with

$$\mathcal{I}_{\lambda}^{T}(\Theta) = n^{2} \left[1 - \left| \cos\left(n\frac{\lambda}{2}\right) \right| \cos\left(\Theta - n\frac{\lambda}{2}\right) \right]^{-1},\tag{47}$$

$$\mathcal{I}_{\lambda}^{\parallel}(\Theta) = n^2 \left| \sin\left(\frac{n\lambda - \Theta}{2}\right) \right|^2 \left[1 - \left| \cos\left(n\frac{\lambda}{2}\right) \right| \cos\left(\Theta - n\frac{\lambda}{2}\right) \right]^{-2}. \tag{48}$$

Here, $\mathcal{I}_{\lambda}^{T}(\Theta)$ attains its maximum for $\Theta_{T} = \underset{\Theta}{\arg\max}\,\mathcal{I}_{\lambda}^{T}(\Theta) = n\frac{\lambda}{2}$ (Pancharatnam phase), whereas the parallel component $\mathcal{I}_{\lambda}^{\parallel}(\Theta)$ vanishes under the condition $\Theta_{\parallel} = \underset{\Theta}{\arg\min}\,\mathcal{I}_{\lambda}^{\parallel}(\Theta) = n\lambda$. Under the small-angle approximation for λ $(n\lambda < 1 \text{ rad})$, the postselection parameter Θ_{\perp} that maximizes $\mathcal{I}_{\lambda}^{\perp}(\Theta)$ is

$$\Theta_{\perp} = \arg\max_{\Theta} \mathcal{I}_{\lambda}^{\perp}(\Theta) = \cos^{-1} \left[\cos^{2}\left(n\frac{\lambda}{2}\right)\right],$$
 (49)

a direct function of the Pancharatnam phase. Figure 3(a) illustrates the trade-off around Pancharatnam phase between $\mathcal{I}_{\lambda}^{\perp}(\Theta)$ and $\mathcal{I}_{\lambda}^{\parallel}(\Theta)$ as Θ varies.

Figure 3(b) shows that the operator $\hat{\mathcal{O}}_{\lambda}^{(0)}=e^{-in\lambda/2}|1\rangle\langle 1|^{\otimes n}+e^{in\lambda/2}|1\rangle\langle 1|^{\otimes n}$, which introduces the same relative phase $n\lambda$ to the meter state, leads to a cooperative behavior between $\mathcal{I}_{\lambda}^{\parallel}(\Theta)$ and $\mathcal{I}_{\lambda}^{T}(\Theta)$ which reduces the total QFI by 83.33%, rendering $\hat{\mathcal{O}}_{\lambda}^{(0)}$ suboptimal. QFI in this case is maximized for $\Theta_{\perp}=\arg\max_{\Omega}\mathcal{I}_{\lambda}^{\perp}(\Theta)=\pm n\frac{\lambda}{2}$.

F. Qudit-enhanced Sensitivity: Boosting \mathcal{T} , $\Delta \lambda$, and SNR

For a qudit meter with d>2, the expectation value $\langle \hat{\mathcal{O}}_{\lambda}^{P} \rangle$ is found to exhibit a characteristic interference pattern, with modulus $|\langle \hat{\mathcal{O}}_{\lambda}^{P} \rangle| = |\sin(dn\lambda/2)|/[d|\sin(n\lambda/2)|]$, and Pancharatnam phase $\mathrm{Im} \ln \langle \hat{\mathcal{O}}_{\lambda}^{P} \rangle = (d-1)n\lambda/2$. This leads to the postselection probability

$$\mathcal{P}_{\lambda}^{(1/2)}(\Theta) = \frac{1}{2} \left[1 - \frac{\sin\left(\frac{dn\lambda}{2}\right)}{d\sin\left(\frac{n\lambda}{2}\right)} \cos\left(\Theta - \frac{(d-1)n\lambda}{2}\right) \right]. \quad (50)$$

From Eq. (27) or (32), the total change $\mathcal{Q}_{\lambda}^T=(d-1)(2d-1)/6$, and the parallel change $\mathcal{Q}_{\lambda}^{\parallel}$ that captures the Θ -optimization ((28) or (33)) gives

$$Q_{\lambda}^{\parallel} = |\mathcal{Z}(\lambda) - e^{i\Theta} \mathcal{Z}_0|^2 / d^2, \tag{51}$$

where $\mathcal{Z}_0 = d(d-1)/2$ and

$$\mathcal{Z}(\lambda) = \sum_{k=0}^{d-1} k e^{ink\lambda} = \frac{e^{in\lambda} - de^{ind\lambda} + (d-1)e^{in(d+1)\lambda}}{\left(1 - e^{in\lambda}\right)^2}.$$

Figure 4(a) shows QFI as functions of Θ for d=30, illustrating how $\hat{\mathcal{O}}_{\lambda}^{P}$ enables precise tuning of the trade-off between orthogonal and parallel sensitivities. The results in Fig. 4(b) reveal that

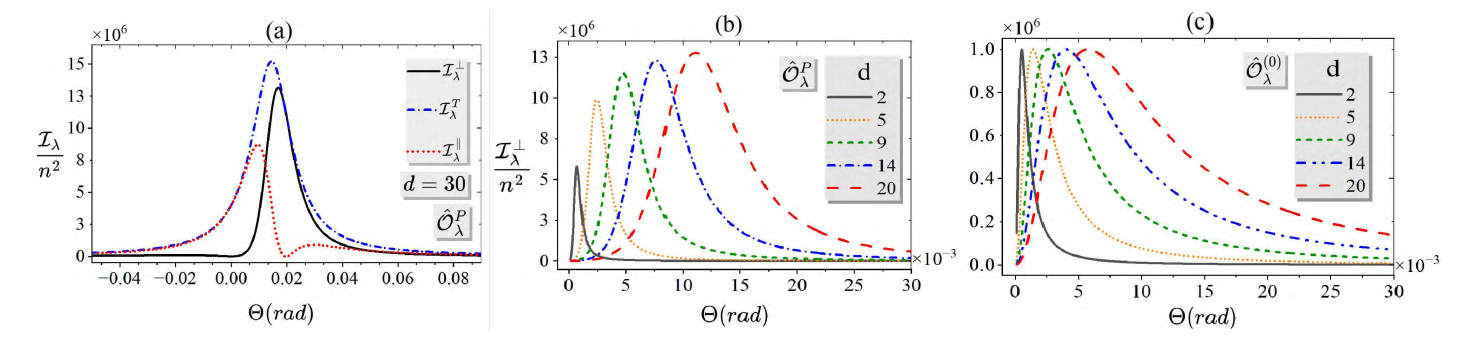


Figure 4. (a) Variation of the normalized QFI $\mathcal{I}_{\lambda}^{\perp}/n^2$, $\mathcal{I}_{\lambda}^{T}/n^2$, and $\mathcal{I}_{\lambda}^{\parallel}/n^2$ as functions of Θ for d=30 and $n\lambda=10^{-3}$, illustrating how the operator $\hat{\mathcal{O}}_{\lambda}^{P}$ enables precise tuning of the trade-off between orthogonal and parallel sensitivities. (b) The normalized QFI $\mathcal{I}_{\lambda}^{1}(\Theta)$ plotted against Θ for various meter dimensions d, demonstrating a pronounced increase in QFI and the formation of sharply localized peaks with rising d when using $\hat{\mathcal{O}}_{\lambda}^{\gamma}$. These peaks signify optimal Θ at which maximal quantum sensitivity is achieved as system complexity grows. (c) In contrast, the QFI $\mathcal{I}_{\lambda}^{\perp}(\Theta)$ corresponding to $\hat{\mathcal{O}}_{\lambda}^{(0)}$ remains essentially unchanged in its maximal numerical value as d increases, reflecting a diminished sensitivity to the meter dimension d.

the QFI associated with the operator $\hat{\mathcal{O}}_{\lambda}^{P}$ exhibits a pronounced upward scaling as the meter dimension d increases. Conversely, Fig. 4(c) shows that the QFI computed with the operator $\hat{\mathcal{O}}_{\lambda}^{(0)}$ yields a QFI that is comparatively insensitive to d.

This stark difference between $\hat{\mathcal{O}}_{\lambda}^{P}$ and $\hat{\mathcal{O}}_{\lambda}^{(0)}$ demonstrates that the presence of Pancharatnam phase in the postselected system is crucial for unlocking the full advantage offered by increasing the meter quantum complexity.

For any qudit meter, the optimal postselection parameter Θ that maximizes the total QFI per trial, \mathcal{T} , is not Θ_{\perp} that maximizes $\mathcal{I}_{\lambda}^{\perp}(\Theta)$. Instead, it is the value of Θ that satisfies the condition $\mathcal{Q}_{\lambda}^{\parallel}=0$, as illustrated in Fig. 5(a). From Eq. (51) this optimal postselection parameter can be expressed analytically as

$$\Theta_{\parallel} = -n\lambda + \operatorname{Im} \ln \left[de^{ind\lambda} - e^{in\lambda} + (1 - d)e^{in(d+1)\lambda} \right], (52)$$

which defines the precise tuning condition for maximizing \mathcal{T} .

Figure 5(b) shows that the uncertainty $\Delta \lambda$ peaks near $\Theta =$ 0, rendering this regime unsuitable for estimation. In contrast, optimizing within the interval $(\Theta_{\perp}, \Theta_{\parallel})$ enables saturation of the Cramér-Rao bound (6), thus achieving optimal measurement precision.

The signal-to-noise ratio (SNR), a fundamental metric quantifying the precision of the estimated parameter λ is defined as SNR = $\langle \lambda \rangle / \sqrt{\text{Var}(\lambda)}$. By the Cramér-Rao bound, the SNR satisfies the inequality

$$SNR \le \langle \lambda \rangle \sqrt{\mathcal{I}_{\lambda}^{\perp}(\Theta)}.$$
 (53)

In the weak coupling regime, and for d=2, the QFI asymptotically behaves as $\mathcal{I}_{\lambda}^{\perp}(\Theta^*) \approx (1+\sqrt{2})^2/\lambda^2$, yielding a maximal SNR for a single measurement of approximately SNR $\lesssim 2.4$. Figure 5(c) demonstrates the potential for further enhancement achievable through the use of qudit meter states in conjunction with the operator $\hat{\mathcal{O}}_{\lambda}^{P}$.

Challenges and Key Considerations for Future Studies

Finally, we delineate three key characteristic values of the postselection parameter Θ

$$\Theta_T = \arg\max_{\Theta} \mathcal{I}_{\lambda}^T(\Theta) = \operatorname{Im} \ln \langle \hat{O}_{\lambda}^P \rangle, \tag{54}$$

$$\Theta_{T} = \underset{\Theta}{\arg \max} \, \mathcal{I}_{\lambda}^{T}(\Theta) = \operatorname{Im} \ln \langle \hat{O}_{\lambda}^{P} \rangle, \tag{54}$$

$$\Theta_{\perp} = \underset{\Theta}{\arg \max} \, \mathcal{I}_{\lambda}^{\perp}(\Theta), \tag{55}$$

$$\Theta_{\parallel} = \underset{\Theta}{\arg\min} \, \mathcal{I}_{\lambda}^{\parallel}(\Theta), \tag{56}$$

each marking distinct operational regimes, with $\Theta_T < \Theta_{\perp} <$ Θ_{\parallel} . Achieving the most accessible enhancement in the quality of quantum compression channels requires the suppression of parallel dynamics precisely at the Pancharatnam phase. This condition leads to the equality

$$\Theta_{\parallel} = \Theta_{\perp} = \operatorname{Im} \ln \langle \hat{O}_{\lambda}^{P} \rangle. \tag{57}$$

Future research should focus on manipulating the Pancharatnam phase and exploring meter operators capable of realizing this critical equality. Detailed investigation into the structural and operational properties of such meter operators is essential to optimize many features of postselected quantum metrology protocols.

To illustrate this point, consider the meter operator

$$\hat{\mathcal{O}}_{\lambda}^{P} = \sum_{k=0}^{d-1} e^{ik^{\epsilon}\lambda} |k\rangle\langle k|, \tag{58}$$

with the fractional exponent approaching zero, $\epsilon \to 0^+$, representing a slowly varying phase. This form leads to the expectation value

$$\langle \hat{O}_{\lambda}^{P} \rangle = \frac{1}{d} \sum_{k=0}^{d-1} e^{i\lambda k^{\epsilon}}.$$
 (59)

This sum is approximated as $\sum_{k=0}^{d-1} e^{i\lambda k^\epsilon} \approx 1 + e^{i\lambda} \sum_{k=1}^{d-1} k^{i\lambda\epsilon}$, where $k^{i\lambda\epsilon} = e^{i\lambda\epsilon\ln(k)}$. Using the integral approximation for

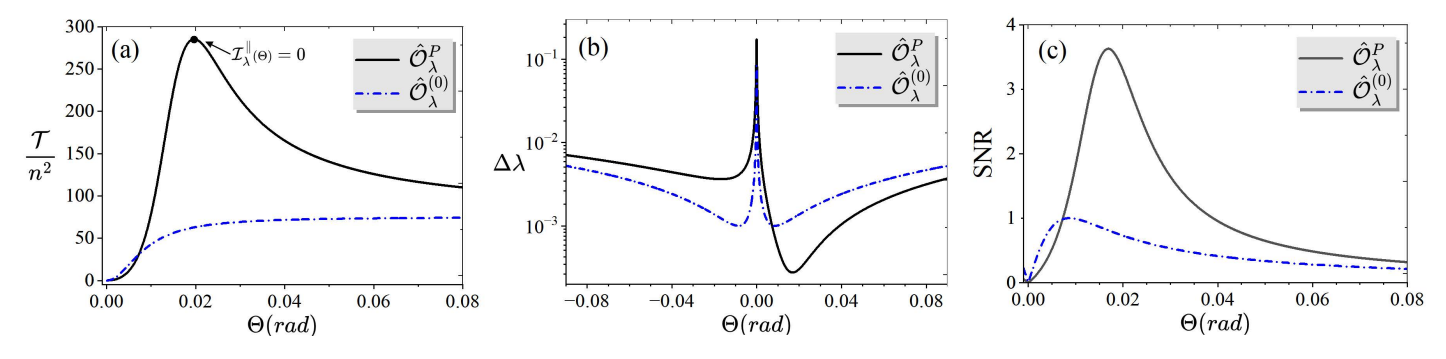


Figure 5. (a) The operator $\hat{\mathcal{O}}_{\lambda}^{P}$ enables a pronounced enhancement of the total QFI per trial \mathcal{T} , reaching its peak at the optimal parameter Θ_{\parallel} , while $\hat{\mathcal{O}}_{\lambda}^{(0)}$ yields consistently lower sensitivity. (b) The estimation uncertainty $\Delta\lambda$ exhibits a sharp increase near $\Theta=0$, indicating suboptimal performance in this regime, whereas optimization within the intermediate interval $(\Theta_{\perp},\Theta_{\parallel})$ achieves minimal uncertainty. (c) The signal-to-noise ratio (SNR) is significantly amplified by $\hat{\mathcal{O}}_{\lambda}^{P}$, attaining its maximum at Θ_{\parallel} , in contrast to the limited case observed for $\hat{\mathcal{O}}_{\lambda}^{(0)}$. The results correspond to d=30 and $n\lambda=10^{-3}$.

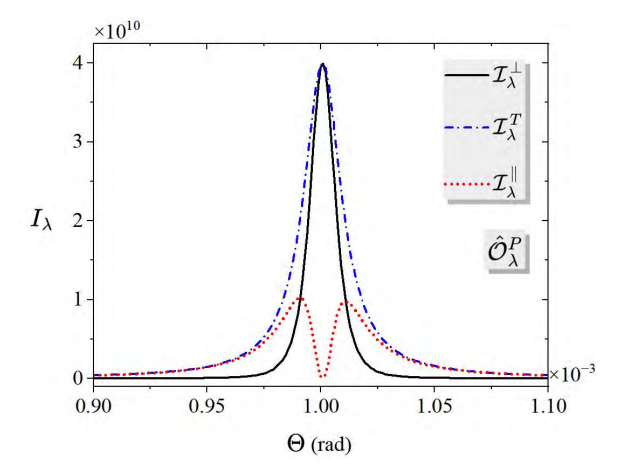


Figure 6. Normalized QFI $\mathcal{I}_{\lambda}^{\perp}$, $\mathcal{I}_{\lambda}^{T}$, and $\mathcal{I}_{\lambda}^{\parallel}$ are plotted as functions of the postselection parameter Θ for $\lambda=10^{-3}$, $d=10^{4}$, and $\epsilon=10^{-4}$. The results demonstrate a pronounced central peak in the total and orthogonal components, signifying optimal quantum sensitivity at the corresponding postselection parameter Θ . The parallel component, by contrast, exhibits a split-peak structure and vanishes at the central phase point, illustrating the complete suppression of nonphysical parallel evolution at the Pancharatnam phase given in Eq. (63).

large d we get [28]

$$\sum_{k=1}^{d-1} k^{i\lambda\epsilon} \approx \int_{1}^{d} x^{i\lambda\epsilon} dx = \frac{d^{1+i\lambda\epsilon} - 1}{1 + i\lambda\epsilon},\tag{60}$$

thus $\sum_{i=0}^{d-1}e^{i\lambda k^\epsilon}pprox 1+e^{i\lambda}rac{d^{1+i\lambda\epsilon}-1}{1+i\lambda\epsilon}$, and the expectation value can be rewritten as

$$\langle \hat{O}^P_{\lambda} \rangle \approx \frac{1}{d} \left[1 + e^{i\lambda} \frac{d^{1+i\lambda\epsilon} - 1}{1 + i\lambda\epsilon} \right] = \frac{1}{d} + e^{i\lambda} \frac{d^{i\lambda\epsilon} - d^{-1}}{1 + i\lambda\epsilon}.$$
 (61)

where $d^{i\lambda\epsilon}=e^{i\lambda\epsilon\ln(d)}\approx 1+i\lambda\epsilon\ln(d)+\ldots$, using the condition $|\lambda\epsilon\ln(d)|\ll 1$, and $\frac{1}{1+i\lambda\epsilon}\approx 1-i\lambda\epsilon-\lambda^2\epsilon^2+\ldots$. This gives

$$\langle \hat{O}_{\lambda}^{P} \rangle \approx e^{i\lambda} \left\{ 1 + i\lambda \epsilon [\ln(d) - 1] \right\} + \frac{1 - e^{i\lambda}}{d} + \dots$$
 (62)

Noting that $\ln(1+\delta) \approx \delta$ for small δ , where $\delta=i\lambda\epsilon[\ln(d)-1]+\frac{e^{-i\lambda}-1}{d}+\ldots$ The Pancharatnam phase gives

$$\operatorname{Im} \ln \langle \hat{O}_{\lambda}^{P} \rangle = \lambda + \lambda \epsilon [\ln(d) - 1] - \frac{\sin \lambda}{d} + \dots$$

$$\approx \lambda [1 - \epsilon + \epsilon \ln(d)] \approx \lambda. \tag{63}$$

As illustrated in Fig. 6, in both the small- ϵ and large-d limits, the equality (57), holds. At this critical phase, the nonphysical parallel evolution is completely eliminated, i.e., $\mathcal{I}_{\lambda}^{\parallel}(\Theta)=0$, while the compression quality achieves its maximum by fully concentrating all accessible information contained in $\mathcal{I}_{\lambda}^{T}(\Theta)$ into the experimentally measurable orthogonal component $\mathcal{I}_{\lambda}^{\perp}(\Theta)$. This demonstrates the Pancharatnam phase acts as a natural, robust benchmark for optimizing compression quality of quantum channels.

V. CONCLUSION

In this work, we have identified the noncyclic Pancharatnam phase as the fundamental geometric criterion governing the optimal operation of quantum compression channels within postselected metrology.

By explicitly connecting the Pancharatnam phase to the delicate interplay between parallel and orthogonal evolutions of the meter state as the estimated parameter varies, we establish a principled framework for optimizing the QFI associated with interaction-strength parameter estimation.

Our analysis demonstrates that even minute deviations from the Pancharatnam phase lead to a significant deterioration in metrological precision, highlighting its critical and practical relevance for experimental realizations. This geometric insight enriches the theoretical foundation of quantum parameter estimation and points toward new avenues for designing robust and efficient quantum sensing protocols that effectively exploit Pancharatnam phase phenomena to achieve quantum advantages in metrology.

SUPPLEMENTARY DERIVATIONS AND DETAILS OF THE THEORETICAL MODEL

Appendix A: Quantum parallel transport condition

A canonical example of parallel transport in classical physics is the transport of a tangent vector along a closed loop on the surface of a sphere. Consider a vector initially defined at point A and transported along the geodesic triangle $A \to B \to C \to A$. Throughout this process, the vector remains confined to the tangent plane of the sphere, and no local rotation (phase accumulation) occurs along the geodesic segments AB, BC, and CA. Upon returning to the initial point A, the vector generally undergoes a net rotation relative to its original orientation, a manifestation of the sphere's intrinsic curvature encoded by the holonomy associated with the loop.

By analogy, the concept of parallel transport extends naturally to the evolution of quantum states in a Hilbert space \mathcal{H} . Quantum states differing only by a global phase factor form equivalence classes known as rays, which correspond to one-dimensional subspaces spanned by normalized vectors. The collection of all such rays constitutes the projective Hilbert space $P\left(\mathcal{H}\right)$, a manifold that effectively removes the physically irrelevant global phase from the state description; see Fig.7. This space can be identified with the set of pure-state density matrices modulo global phase, serving as the natural arena for geometric phases and holonomies in quantum mechanics.

The quantum parallel transport condition can be rigorously formulated to ensure the absence of any geometric phase accumulation as the parameter λ varies infinitesimally. Concretely, this condition requires that no relative phase is introduced between the states $|\Psi_{\lambda}\rangle$ and $|\Psi_{\lambda+d\lambda}\rangle$, which is mathematically equivalent to demanding that their overlap $\langle\Psi_{\lambda}\,|\Psi_{\lambda+d\lambda}\rangle$ remains strictly real and positive. The argument of this overlap, defined as $\arg{\langle\Psi_{\lambda}\,|\Psi_{\lambda+d\lambda}\rangle}=\mathrm{Im}\ln{\langle\Psi_{\lambda}\,|\Psi_{\lambda+d\lambda}\rangle}$ vanishes identically. Accordingly

$$\begin{split} \operatorname{Im} \operatorname{Ln} \left\langle \Psi_{\lambda} \left| \Psi_{\lambda + d\lambda} \right. \right\rangle &= \operatorname{Im} \operatorname{Ln} \left(\left\langle \Psi_{\lambda} \middle| \Psi_{\lambda} \right\rangle \right. \\ &+ \left\langle \Psi_{\lambda} \middle| \partial_{\lambda} \Psi_{\lambda} \right\rangle d\lambda + O(d\lambda^{2}) \right) \\ &\simeq \operatorname{Im} \operatorname{Ln} \left(1 + \left\langle \Psi_{\lambda} \middle| \partial_{\lambda} \Psi_{\lambda} \right\rangle d\lambda \right) \\ &\simeq \left\langle \Psi_{\lambda} \middle| \partial_{\lambda} \Psi_{\lambda} \right\rangle d\lambda = 0. \end{split}$$

and the quantum parallel transport condition can be expressed by $\langle \Psi_{\lambda}|\partial_{\lambda}\Psi_{\lambda}\rangle=0,$ which imposes that the tangent vector $|\partial_{\lambda}\Psi_{\lambda}\rangle$ remains orthogonal to the state vector $|\Psi_{\lambda}\rangle$ in Hilbert space, i.e., $|\partial_{\lambda}\Psi_{\lambda}\rangle\perp|\Psi_{\lambda}\rangle.$ This orthogonality condition defines a horizontal lift of the parameterized curve from the projective Hilbert space to the full Hilbert space, eliminating gauge-dependent dynamical phase contributions.

Appendix B: Geometrical description of the QFI

When a quantum state $|\Psi_{\lambda}\rangle$ exhibits parametric dependence on λ , its derivative $|\partial_{\lambda}\Psi_{\lambda}\rangle$ describes the state infinitesimal variations. These variations encompass two distinct contributions: (i) a physical component reflecting the state's evolution to a

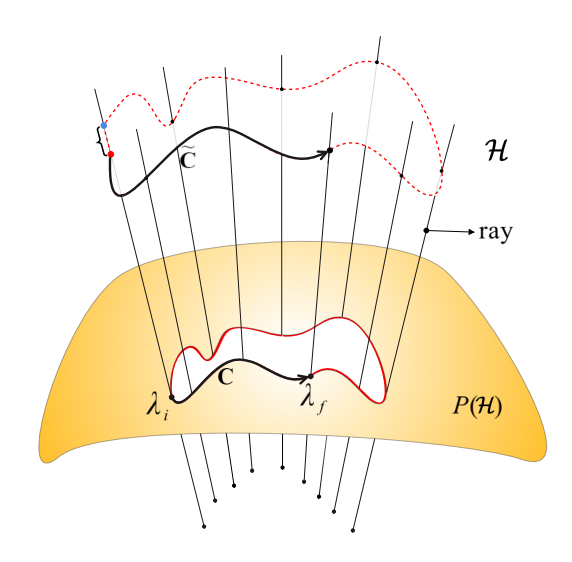


Figure 7. The set of all equivalent state vectors (a ray) represents a point in the projective Hilbert space $P(\mathcal{H})$.

different ray within the projective Hilbert space, and (ii) a gauge-dependent component corresponding to an infinitesimal phase rotation, which is parallel to $|\Psi_{\lambda}\rangle$. Thus, the derivative with respect to the parameter λ decomposes as:

$$|\partial_{\lambda}\Psi_{\lambda}\rangle = |\partial_{\lambda}\Psi_{\lambda}^{\parallel}\rangle + |\partial_{\lambda}\Psi_{\lambda}^{\perp}\rangle. \tag{B1}$$

The component of $|\partial_{\lambda}\Psi_{\lambda}\rangle$ parallel to $|\Psi_{\lambda}\rangle$ is given by

$$|\partial_{\lambda}\Psi_{\lambda}^{\parallel}\rangle = \mathbb{P}_{\psi} |\partial_{\lambda}\Psi_{\lambda}\rangle = |\Psi_{\lambda}\rangle \langle \Psi_{\lambda}| \partial_{\lambda}\Psi_{\lambda}\rangle,$$

where $\mathbb{P}_{\psi} = |\Psi_{\lambda}\rangle \langle \Psi_{\lambda}|$ is the projector onto the state $|\Psi_{\lambda}\rangle$. The overlap $\langle \Psi_{\lambda}| \, \partial_{\lambda} \Psi_{\lambda} \rangle$ causes a global phase change that do not affect measurements outcomes. The orthogonal component is derived simply by subtraction of the parallel component from $|\partial_{\lambda} \Psi_{\lambda}\rangle$ and can be written as

$$\begin{aligned} |\partial_{\lambda}\Psi_{\lambda}^{\perp}\rangle &= |\partial_{\lambda}\Psi_{\lambda}\rangle - |\partial_{\lambda}\Psi_{\lambda}^{\parallel}\rangle \\ &= (\mathbb{I} - |\Psi_{\lambda}\rangle\langle\Psi_{\lambda}|)|\partial_{\lambda}\Psi_{\lambda}\rangle, \end{aligned} \tag{B2}$$

which leads to observable differences in the quantum state. The decomposition (B1) of the state derivative becomes

$$|\partial_{\lambda}\Psi_{\lambda}\rangle = \underbrace{\langle\Psi_{\lambda}|\partial_{\lambda}\Psi_{\lambda}\rangle|\Psi_{\lambda}\rangle}_{\text{Parallel (global phase)}} + \underbrace{(\mathbb{I} - |\Psi_{\lambda}\rangle\langle\Psi_{\lambda}|)|\partial_{\lambda}\Psi_{\lambda}\rangle}_{\text{Orthogonal (physical)}}, \quad (B3)$$

which clearly isolates the physically relevant sensitivity of the state to λ . The QFI can then be written as

$$\mathcal{I}_{\lambda}^{\perp} = 4\langle \partial_{\lambda} \Psi_{\lambda}^{\perp} | \partial_{\lambda} \Psi_{\lambda}^{\perp} \rangle
= 4(\langle \partial_{\lambda} \Psi_{\lambda} | \partial_{\lambda} \Psi_{\lambda} \rangle - |\langle \Psi_{\lambda} | \partial_{\lambda} \Psi_{\lambda} \rangle|^{2})$$
(B4)

$$= \! 4 \big(\big\| |\partial_{\lambda} \Psi_{\lambda} \rangle \big\|^{2} \! - \! \big\| |\partial_{\lambda} \Psi_{\lambda}^{\parallel} \rangle \big\|^{2} \big), \tag{B5}$$

which rigorously quantifies the parametric sensitivity of a quantum state by evaluating the squared norm of the component of

the state's derivative that is orthogonal to the state vector itself in Hilbert space. This orthogonal component encapsulates the physically meaningful variation of the state within the projective Hilbert space, effectively filtering out gauge-dependent phase fluctuations parallel to the state vector. Consequently, the QFI serves as a fundamental metric governing the ultimate attainable precision in parameter estimation, as formalized by the quantum Cramér-Rao bound.

Appendix C: Gauge invariance of QFI

By performing a phase redefinition (gauge transformation) for the quantum state

$$|\Psi_{\lambda}\rangle \to e^{i\phi_{\lambda}}|\Psi_{\lambda}\rangle,$$

where ϕ_{λ} is an arbitrary real function. The total derivative reads

$$|\partial_{\lambda}\Psi_{\lambda}\rangle \rightarrow e^{i\phi_{\lambda}}(i|\Psi_{\lambda}\rangle\partial_{\lambda}\phi_{\lambda} + |\partial_{\lambda}\Psi_{\lambda}\rangle),$$

and its norm gives

$$\begin{aligned} \left\| \left| \partial_{\lambda} \Psi_{\lambda} \right\rangle \right\|^{2} &\to \left\langle \partial_{\lambda} \Psi_{\lambda} \right| \partial_{\lambda} \Psi_{\lambda} \right\rangle + (\partial_{\lambda} \phi_{\lambda})^{2} \\ &+ 2i \partial_{\lambda} \phi_{\lambda} \left\langle \Psi_{\lambda} \right| \partial_{\lambda} \Psi_{\lambda} \right\rangle, \end{aligned} \tag{C1}$$

where $\langle \Psi_{\lambda} | \Psi_{\lambda} \rangle = 1$. The parallel term transforms as

$$\begin{split} \left\| |\partial_{\lambda} \Psi_{\lambda}^{\parallel} \rangle \right\|^{2} &\rightarrow |\langle \Psi_{\lambda} | \partial_{\lambda} \Psi_{\lambda} \rangle + i \partial_{\lambda} \phi_{\lambda}|^{2} \\ &= |\langle \Psi_{\lambda} | \partial_{\lambda} \Psi_{\lambda} \rangle|^{2} + (\partial_{\lambda} \phi_{\lambda})^{2} \\ &+ 2i \partial_{\lambda} \phi_{\lambda} \langle \Psi_{\lambda} | \partial_{\lambda} \Psi_{\lambda} \rangle. \end{split} \tag{C2}$$

Substitute the last two expressions into the QFI formula (7), we find that the quantities involving ϕ_{λ} cancel exactly

$$\mathcal{I}_{\lambda}^{\perp} = 4\langle \partial_{\lambda} \Psi_{\lambda} | \partial_{\lambda} \Psi_{\lambda} \rangle - 4|\langle \Psi_{\lambda} | \partial_{\lambda} \Psi_{\lambda} \rangle|^{2}. \tag{C3}$$

The QFI formula is gauge-invariant.

Appendix D: Derivation of the QFI associated with $|\Psi_{\lambda}(\Theta)\rangle$

To derive the QFI formula, we start from the compressed state

$$|\Psi_{\lambda}(\Theta)\rangle = \mathcal{P}_{\lambda}^{-1/2}(\Theta)|\mathcal{S}_{f}\rangle \otimes \hat{\mathbb{K}}_{\lambda}(\Theta)|\mathcal{M}_{i}\rangle = |\mathcal{S}_{f}\rangle \otimes |\Phi_{\lambda}(\Theta)\rangle\,, \tag{D1}$$

and find its derivative

$$\left|\partial_{\lambda}\Phi_{\lambda}(\Theta)\right\rangle = \mathcal{P}_{\lambda}^{-1/2}(\Theta)\left[\partial_{\lambda}\hat{\mathbb{K}}_{\lambda}(\Theta) - \frac{1}{2}\hat{\mathbb{K}}_{\lambda}(\Theta)\partial_{\lambda}\mathrm{Log}\mathcal{P}_{\lambda}(\Theta)\right]\left|\mathcal{M}_{i}\right\rangle. \tag{D2}$$

Thus, the magnitude of the total derivative is given by

$$\begin{split} \left\| |\partial_{\lambda} \Psi_{\lambda}(\Theta) \rangle \right\|^{2} &= \mathcal{P}_{\lambda}^{-1}(\Theta) \left[\left\langle \partial_{\lambda} \hat{\mathbb{K}}_{\lambda}^{\dagger}(\Theta) \partial_{\lambda} \hat{\mathbb{K}}_{\lambda}(\Theta) \right\rangle \\ &- \frac{\mathcal{P}_{\lambda}^{-1}(\Theta)}{2} \left\langle \partial_{\lambda} \left(\hat{\mathbb{K}}_{\lambda}^{\dagger}(\Theta) \hat{\mathbb{K}}_{\lambda}(\Theta) \right) \right\rangle \partial_{\lambda} \text{Log} \mathcal{P}_{\lambda}(\Theta) \right] \\ &+ \frac{1}{4} \left(\partial_{\lambda} \text{Log} \mathcal{P}_{\lambda}(\Theta) \right)^{2}. \end{split} \tag{D3}$$

Using expressions (D1) and (D2) one can find

$$\begin{split} \left\langle \, \Phi_{\lambda}(\Theta) \middle| \partial_{\lambda} \Phi_{\lambda}(\Theta) \right\rangle = & \mathcal{P}_{\lambda}^{-1}(\Theta) \, \left\langle \, \hat{\mathbb{K}}_{\lambda}^{\dagger}(\Theta) \partial_{\lambda} \hat{\mathbb{K}}_{\lambda}(\Theta) \right\rangle \\ & - \frac{1}{2} \partial_{\lambda} \mathrm{Log} \mathcal{P}_{\lambda}(\Theta), \end{split} \tag{D4}$$

$$\begin{split} \langle \, \partial_{\lambda} \Phi_{\lambda}(\Theta) \big| \Phi_{\lambda}(\Theta) \rangle = & \mathcal{P}_{\lambda}^{-1}(\Theta) \, \langle \, \partial_{\lambda} \hat{\mathbb{K}}_{\lambda}^{\dagger}(\Theta) \hat{\mathbb{K}}_{\lambda}(\Theta) \rangle \\ & - \tfrac{1}{2} \partial_{\lambda} \mathrm{Log} \mathcal{P}_{\lambda}(\Theta), \end{split} \tag{D5}$$

and the parallel term in the QFI gives

$$\begin{split} \left\| |\partial_{\lambda} \Psi_{\lambda}^{\parallel}(\Theta) \rangle \right\|^{2} = & \mathcal{P}_{\lambda}^{-2}(\Theta) \left| \left\langle \hat{\mathbb{K}}_{\lambda}^{\dagger}(\Theta) \, \partial_{\lambda} \hat{\mathbb{K}}_{\lambda}(\Theta) \right\rangle \right|^{2} \\ & - \frac{\mathcal{P}_{\lambda}^{-1}(\Theta)}{2} \left\langle \partial_{\lambda} \big(\hat{\mathbb{K}}_{\lambda}^{\dagger}(\Theta) \hat{\mathbb{K}}_{\lambda}(\Theta) \big) \right\rangle \partial_{\lambda} \text{Log} \mathcal{P}_{\lambda}(\Theta) \\ & + \frac{1}{4} (\partial_{\lambda} \text{Log} \mathcal{P}_{\lambda}(\Theta))^{2}. \end{split} \tag{D6}$$

The final form of the QFI becomes

$$\begin{split} \mathcal{I}_{\lambda}^{\perp} = & 4 \big[\big\| \big| \partial_{\lambda} \Psi_{\lambda}(\Theta) \big\rangle \big\|^{2} - \big\| \big| \partial_{\lambda} \Psi_{\lambda}^{\parallel}(\Theta) \big\rangle \big\|^{2} \big] \\ = & 4 \mathcal{P}_{\lambda}^{-2}(\Theta) \big[\big\langle \partial_{\lambda} \hat{\mathbb{K}}_{\lambda}^{\dagger}(\Theta) \partial_{\lambda} \hat{\mathbb{K}}_{\lambda}(\Theta) \big\rangle \, \mathcal{P}_{\lambda}(\Theta) \\ & - \big| \big\langle \hat{\mathbb{K}}_{\lambda}^{\dagger}(\Theta) \, \partial_{\lambda} \hat{\mathbb{K}}_{\lambda}(\Theta) \big\rangle \big|^{2} \big], \end{split} \tag{D7}$$

which is the QFI written as a function of the channel operator $\hat{\mathbb{K}}_{\lambda}(\Theta)$.

Appendix E: Noncyclic Pancharatnam Phase

To elucidate the nature of the Pancharatnam phase in Eq. (31), we exploit its characteristic non-transitivity [20], which directly reflects the geometric origin of the phase difference. Specifically, we consider the evolution generated by the operator $\hat{\mathcal{O}}_{\lambda}$ as a sequence of j discrete transitions between neighboring states, defined by parameters λ with $\lambda_1=d\lambda,\lambda_2=\lambda_1+d\lambda,\ldots,\lambda_j=\lambda_{j-1}+d\lambda.$ The phase difference between the initial and final states is then constructed via successive projections: the initial state $|\phi_1\rangle$ is projected onto the second state $|\phi_2\rangle\langle\phi_2|\phi_1\rangle$, the second onto the third, and so forth, until the final projection onto the original state $|\phi_1\rangle\langle\phi_1|\phi_j\rangle$. Consequently, the final state is expressed as

$$|\widetilde{\phi}_1\rangle = |\phi_1\rangle\langle\phi_1|\phi_j\rangle\langle\phi_j|\dots\langle\phi_4|\phi_3\rangle\langle\phi_3|\phi_2\rangle\langle\phi_2|\phi_1\rangle, \quad (E1)$$

which differs from the initial state $|\psi_1\rangle$, by the phase factor

$$\begin{split} \theta_{geo} = & \operatorname{Im} \ln \left[\langle \phi_1 | \phi_j \rangle \langle \phi_j | \dots \langle \phi_4 | \phi_3 \rangle \langle \phi_3 | \phi_2 \rangle \langle \phi_2 | \phi_1 \rangle \right] \\ = & \operatorname{Im} \ln \left[\operatorname{Tr} \left(|\phi_j \rangle \langle \phi_j | \dots \langle \phi_3 | \phi_2 \rangle \langle \phi_2 | \phi_1 \rangle \langle \phi_1 | \right) \right] \\ = & \operatorname{Im} \ln \left[\operatorname{Tr} \prod_{k=1}^j \varrho_k \right] \end{split} \tag{E2}$$

corresponds to the geometric phase, which is a gauge-invariant quantity for cyclic evolution, where the initial and final states coincide. In contrast, for noncyclic evolution [29], the final state $|\phi_i\rangle$, does not project back onto the initial state $|\phi_1\rangle$, and the

geometric phase can be generalized accordingly as

$$\begin{split} \theta_{geo} &= \operatorname{Im} \ln \left[\langle \phi_1 | \phi_j \rangle \langle \phi_j | \dots \langle \phi_4 | \phi_3 \rangle \langle \phi_3 | \phi_2 \rangle \langle \phi_2 | \phi_1 \rangle \right] \\ &= \operatorname{Im} \ln \langle \phi_1 | \phi_j \rangle - \operatorname{Im} \ln \prod_{k=1}^{j-1} \langle \phi_k | \phi_{k+1} \rangle \\ &\approx \operatorname{Im} \ln \langle \phi_1 | \phi_j \rangle - \operatorname{Im} \sum_{k=1}^{j-1} \ln \left[1 + \left\langle \phi_k | \partial_\lambda \phi_k \right\rangle d\lambda + \dots \right] \\ &\approx \operatorname{Im} \ln \langle \phi_1 | \hat{\mathcal{O}}_\lambda | \phi_1 \rangle - \operatorname{Im} \sum_{k=1}^{j-1} \left\langle \phi_k | \partial_\lambda \phi_k \right\rangle d\lambda, \end{split} \tag{E3}$$

where $\mathrm{Im} \ln \langle \phi_1 | \phi_j \rangle = \mathrm{Im} \ln \langle \hat{\mathcal{O}}_{\lambda} \rangle$ is the total phase difference between initial and final states. The second term involving $\mathrm{Im} \sum_{k=1}^{j-1} \langle \phi_k | \partial_{\lambda} \phi_k \rangle d\lambda$ is the total dynamical phase. In the limit

 $j \to \infty$, the geometric phase becomes

$$\begin{split} \theta_{geo} &= \operatorname{Im} \ln \langle \hat{\mathcal{O}}_{\lambda} \rangle - \underset{j \to \infty}{\operatorname{Lim}} \big\{ \operatorname{Im} \sum_{k=1}^{j-1} \big\langle \phi_{k} | \partial_{\lambda} \phi_{k} \big\rangle d\lambda \\ &= \operatorname{Im} \ln \langle \hat{\mathcal{O}}_{\lambda} \rangle - \operatorname{Im} \int_{\mathcal{C}} \big\langle \hat{\mathcal{O}}_{\lambda}^{\dagger} \partial_{\lambda} \hat{\mathcal{O}}_{\lambda} \big\rangle d\lambda \\ &= \theta_{tot} - \theta_{dyn}, \end{split} \tag{E4}$$

where the integral is taken along the evolution path $\mathcal C$ in projective Hilbert space $P(\mathcal H)$, the space of density matrices ϱ . This generalization preserves gauge invariance and extends the notion of the Pancharatnam phase beyond cyclic trajectories. When the parallel transport condition $\langle \, \hat{\mathcal O}_{\lambda}^{\dagger} \, \partial_{\lambda} \hat{\mathcal O}_{\lambda} \, \rangle \to 0$ is achieved (see Appendix A), the noncyclic Pancharatnam phase θ_{tot} becomes purely geometric. Figure 2(a) shows the postselection probability $\mathcal P_{\lambda}^{(j)}$ as a function of Θ for the case of $\hat{\mathcal O}_{\lambda}^P$ for different j values. All curves are uniformly phase-shifted, resulting in coincident fringe positions that are independent of j.

- [1] M. A. Taylor and W. P. Bowen, Phys. Rep. 615, 1 (2016).
- [2] V. Giovannetti, S. Lloyd, and L. Maccone, Nat. Photon. 5, 222 (2011).
- [3] L. Pezzè et al., Rev. Mod. Phys. 90, 035005 (2018).
- [4] D. DeMille et al., Nat. Phys. 20, 741 (2024).
- [5] S.-M. Wu et al., Eur. Phys. J. C 84, 1228 (2024).
- [6] D. R. M. Arvidsson-Shukur et al., Nat. Commun. 11, 3775 (2020).
- [7] F. Salvati et al., Phys. Rev. A 110, 022426 (2024).
- [8] J. Yang, Phys. Rev. Lett. 132, 250802 (2024).
- [9] J. Dressel et al., Phys. Rev. A 88, 023821 (2013).
- [10] J. Harris, R. W. Boyd, and J. S. Lundeen, Phys. Rev. Lett. 118, 070802 (2017).
- [11] M. Hallaji, , et al., Nat. Phys. 13, 540 (2017).
- [12] A. Rostom, Ann. Phys. (Berlin) 534, 2100434 (2022).
- [13] S. Lloyd et al., Phys. Rev. Lett. 106, 040403 (2011).
- [14] A. V. Shepelin et al., J. Phys. Conf. Ser. 2081, 012029 (2021).
- [15] D. R. M. Arvidsson-Shukur, A. G. McConnell, and N. Yunger Halpern, Phys. Rev. Lett. 131, 150202 (2023).
- [16] J. Yang, (2024), arXiv:2405.00405 [quant-ph].
- [17] Z.-R. Zhong et al., (2024), arXiv:2412.04838 [quant-ph].
- [18] J. Zhu et al., Appl. Phys. Rev. 12, 021315 (2025).

- [19] S. Pancharatnam, Proc. Indian Acad. Sci. A 44, 247 (1956).
- [20] M. V. Berry, J. Mod. Opt. **34**, 1401 (1987).
- [21] P. Larsson and E. Sjögvist, Phys. Rev. A 68, 042109 (2003).
- [22] J. C. Loredo et al., Phys. Rev. A 80, 012113 (2009).
- [23] T. S. Yakovleva et al., Quantum Electron. 49, 439 (2019).
- [24] A. Rostom, Fortschr. Phys. **71**, 2200122 (2023).
- [25] Under weak interaction, the system and meter become non-maximally entangled, a state expected to suppress the quantum advantage typically offered by maximally entangled states [30].
- [26] P. Kok and B. W. Lovett, Introduction to Optical Quantum Information Processing (Cambridge University Press, 2010).
- [27] Here, the meter can be interpreted as an environmental degree of freedom interacting with the system [31, 32].
- [28] In this regime of small- ϵ and large-d limits, \mathcal{T} asymptotically approaches unity, presenting a nuanced challenge when employing such mathematical operators in Eq. 58.
- [29] N. Mukunda and R. Simon, Ann. Phys-new. York. 228, 205 (1993).
- [30] S.-M. Wu and S.-H. Li, Eur. Phys. J. C 85, 614 (2025).
- [31] E. Sjögvist et al., Phys. Rev. Lett. 85, 2845 (2000).
- [32] T. S. Yakovleva et al., Quantum Stud. Math. Found. 6, 217 (2019).

ACKNOWLEDGMENTS

The authors thank Prof. Leonid Il'ichov for valuable discussions. This work was supported by the State Order (project 124041700105-5) at the Institute of Automation and Electrometry SB RAS.